Theoretical study of electron collisions with the CF_2 radical

M.-T. Lee,[1] I. Iga,[1] L. E. Machado,[2] L. M. Brescansin,[3] E. A. y Castro,[2] and G. L. C. de Souza[1]
[1]*Departamento de Química, UFSCar, 13565-905 São Carlos, São Paulo, Brazil*
[2]*Departamento de Física, UFSCar, 13565-905 São Carlos, São Paulo, Brazil*
[3]*Instituto de Física "Gleb Wataghin," UNICAMP, 13083-970 Campinas, São Paulo, Brazil*
(Received 7 July 2006; published 29 November 2006)

In this work, a theoretical study on electron-CF_2 collisions in the low and intermediate energy range is reported. More specifically, calculated elastic differential, integral and momentum transfer cross sections, as well as total absorption cross sections are presented in the (1–500) eV energy range. A complex optical potential is used to represent the electron-molecule interaction dynamics, whereas the iterative Schwinger variational method combined with the distorted-wave approximation is used to solve the scattering equations. A comparison of the present results is made with the available theoretical and experimental results for electron collisions with CF_2 as well as with O_3 (an isoelectronic molecule of CF_2).

DOI: 10.1103/PhysRevA.74.052716 PACS number(s): 34.80.Bm

I. INTRODUCTION

The interest in electron interaction with highly reactive radicals such as CF_x, SiF_x, $(x=1,2,3)$, etc., has grown recently, in view of their importance in developing plasma devices. It is well known that the plasma environment is composed of many species such as electrons, molecules (in their ground and excited states), neutral radicals, ionic fragments, etc. The knowledge of cross sections for electron interaction with these constituents is important in determining the plasma properties and therefore is useful for plasma modeling. In this sense, cross sections for e^--CF_x $(x=1,2,3)$ collisions are particularly relevant since CF_x are important chemically active products formed in a plasma environment during the etching process of wafers. These species are in fact responsible for etching when carbon perfluoride compounds with general formulas C_nF_{2n+2} are used as feedstock gases. When bombarded by electrons, such compounds may fragment into various CF_x radicals, about which very little is known, particularly their interaction with electrons. The experimental determination of cross sections for e^--CF_x collisions is difficult. So far, only a few experimental cross sections for electron-impact ionization of these reactive radicals were reported in the literature [1,2]. Therefore, theoretical calculations of various cross sections for e^--CF_x $(x=1,2,3)$ collisions would contribute to fulfill this lack. Despite that, only very few theoretical investigations on electron collisions with the CF_x radical have been reported in the literature. In 1999, studies on electron scattering by the CF_3 radical were reported by Diniz *et al.* [3] in the (3–30) eV range using the Schwinger multichannel method. Electron scattering by CF in the (1–500) eV energy range was studied by Lee *et al.* in 2002 [4] using the iterative Schwinger variational method (ISVM). Recently, grand-total (TCS's) and total ionization (TICS's) cross sections for electron collisions with several fluorocarbons, including the CF_x $(x=1,2,3)$ radicals, were calculated in the (20–2000) eV energy range by Antony *et al.* [5] using the so-called group additivity method [6]. In addition, cross sections for low-energy electron collisions with the CF_x $(x=1,2,3)$ radicals were also reported by Rozum *et al.* [7–10] and Rozum and Tennyson [11] using the *R*-matrix method. In their works, elastic and excitation cross sections were reported for incident energies up to 10 eV. Particularly for CF_2, their elastic integral (ICS's) [7] and momentum-transfer (MTCS's) cross sections [10] exhibit a very sharp resonance feature, centered at around 0.95 and 0.88 eV, respectively. However, the occurrence of such a resonance was neither observed in the *R*-matrix ICS's for electron scattering by CF [9] and CF_3 [8] radicals nor in the calculated ICS's [12,13] and experimental total cross sections (TCS's) [14] for electron scattering by ozone, an isoelectronic molecule of CF_2. It is well known that sharp resonances appear quite commonly in ICS's and TCS's for low-energy electron scattering by linear targets such as N_2, C_2H_2, etc. Nevertheless, such an occurrence is rare for nonlinear targets and therefore deserves further investigations.

In this work, we present a theoretical study on electron scattering by the CF_2 radical in the low- and intermediate-energy range. Specifically, calculated elastic differential (DCS's), integral, and momentum-transfer cross sections, as well as total absorption cross sections (TACS's) are presented for electron-impact energies ranging from 0.5 to 500 eV. In our study, a complex optical potential was used to describe the dynamics of e^--CF_2 interaction, whereas a combination of the ISVM [15,16] and the distorted-wave approximation (DWA) [17–20] is used to solve the scattering equations. This procedure has been successfully applied to treat electron scattering by a number of molecules [21–24] and thus we expect that it can also be useful for e^--radical collisions. Although the present method is unable to calculate directly TICS's, our calculated TACS's provide an estimate of the contributions of all inelastic collisions, including both excitation and ionization processes. Joshipura *et al.* [25] have observed that for a set of light molecules the ionization dominates the inelastic processes, the values of the TICS's being about 80% of the TACS's at energies around 100 eV and about 100% for energies above 300 eV. Particularly for the e^--CF_2 collision, some light could be shed through the comparison with the corresponding process for CF_4. For the latter, Christophorou and Olthoff [26] have observed that the values of the TICS's also correspond to about 80% of the TACS's for incident energies above 50 eV. Therefore, the

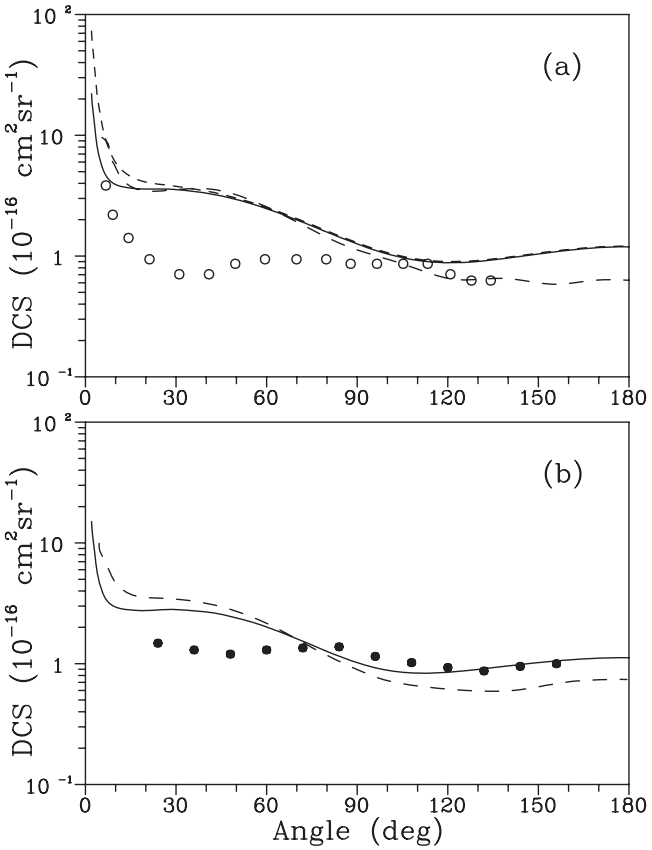

FIG. 1. DCS's for elastic e^--CF_2 scattering at (a) 2 eV and (b) 3 eV. Full curve: present rotationally summed results using the theoretical dipole moment; short-dashed line: present results calculated using the experimental μ; dashed line, calculated DCS's of Rozum and Tennyson [11] using the *R*-matrix method; open circles: experimental data of Allan *et al.* [28]; full circles: experimental data of Shyn and Sweeney [27], both for elastic e^--O_3 collisions.

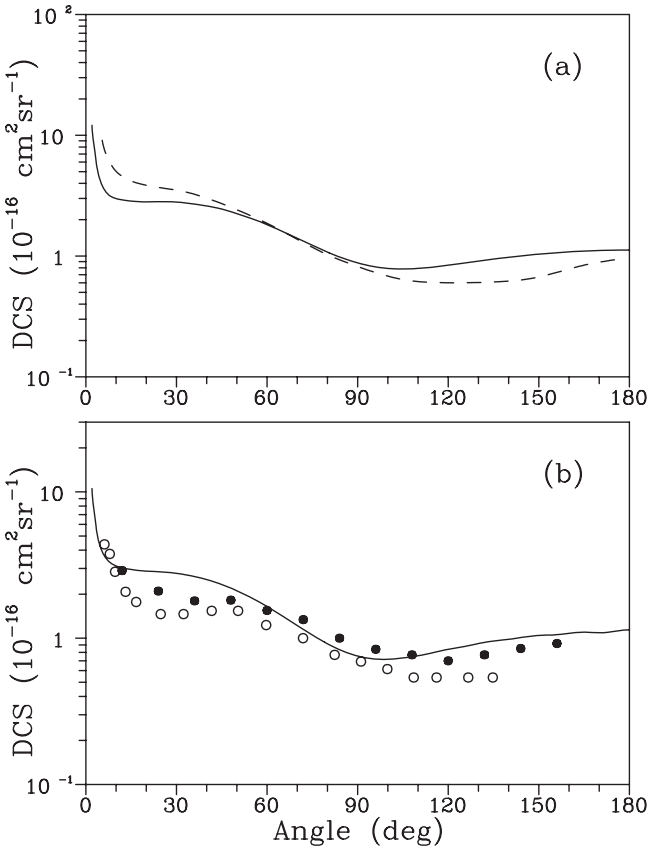

FIG. 2. Same as in Fig. 1, but for (a) 4 eV and (b) 5 eV.

present calculated TACS's provide an upper limit of the TICS's for this radical and their comparison with experimental and calculated TICS's is expected to be meaningful. Due to the lack of experimental cross sections other than TICS's for e^--CF_2 collisions, we also compare our calculated results with the experimental [27,28] and calculated data [29] for electron scattering by O_3.

The organization of this paper is as follows: in Sec. II, we describe briefly the theory used and also give some details of the calculation. In Sec. III, we compare our calculated results with experimental and theoretical data for e^--CF_2 and e^--O_3 scatterings available in the literature. A brief conclusion remark is also presented in that section.

II. THEORY AND CALCULATION

In this section we will briefly discuss the method used; details of the ISVM and the DWA can be found elsewhere [15–19]. Within the adiabatic-nuclei-rotation framework, the DCS's for the excitation for an asymmetric-top rotor from an initial rotational level $J\tau$ to a final level $J'\tau'$ is given by

$$\frac{d\sigma}{d\Omega}(J\tau \to J'\tau') = \frac{1}{(2J+1)}\frac{k}{k_0}\sum_{M=-J}^{J}\sum_{M'=-J'}^{J'}|f_{J\tau M\to J'\tau' M'}|^2, \tag{1}$$

where k_0 and k are the magnitudes of the initial and final linear momenta of the scattering electrons, respectively, $f_{J\tau M\to J'\tau' M'}$ is the rotational excitation scattering amplitude related to the target rotational eigenfunctions by

$$f_{J\tau M\to J'\tau' M'} = \langle \Psi_{J'\tau' M'}(\Omega)|f^{LF}|\Psi_{J\tau M}(\Omega)\rangle, \tag{2}$$

and $\Omega \equiv (\alpha, \beta, \gamma)$ are the Euler angles defining the direction of the target principal axes in the laboratory frame (LF). The eigenfunctions $\Psi_{J\tau M}(\Omega)$ appearing in Eq. (2) are written as linear combinations of symmetric-top eigenfunctions [30],

$$\Psi_{J\tau M}(\Omega) = \sum_{K=-J}^{J} a_{KM}^{J\tau}\Phi_{JKM}(\Omega), \tag{3}$$

where the symmetric-top eigenfunctions are given by

$$\Phi_{JKM}(\Omega) = \left(\frac{2J+1}{8\pi^2}\right)D_{KM}^{J^*}(\Omega), \tag{4}$$

and D_{KM}^{J} are the well-known Wigner rotation matrices [31]. Also, f^{LF} appearing in Eq. (2) is the electronic part of the LF scattering amplitude, which can be related to the corresponding body-frame (BF) T matrix by a usual frame transforma-

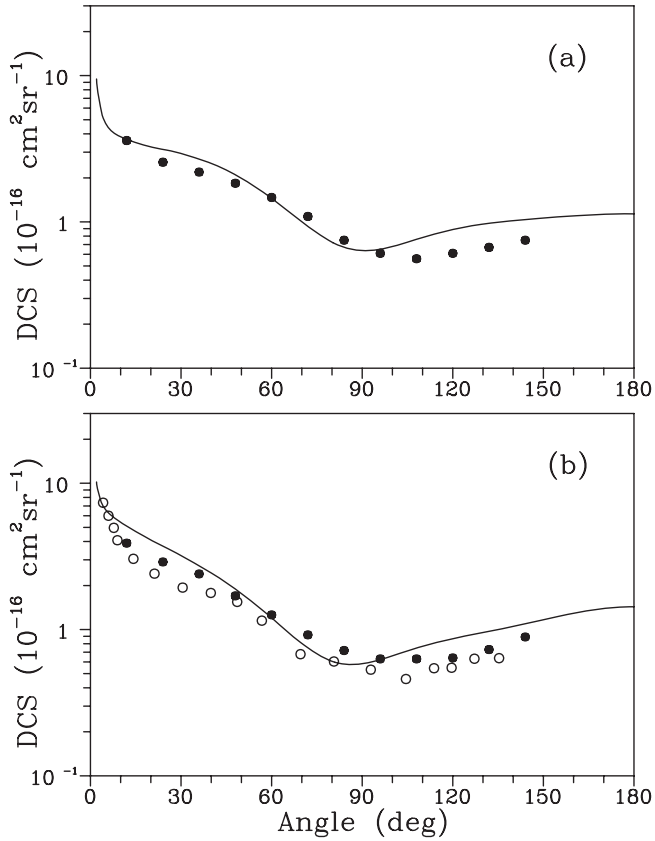

FIG. 3. Same as in Fig. 1, but for (a) 7 eV and (b) 10 eV.

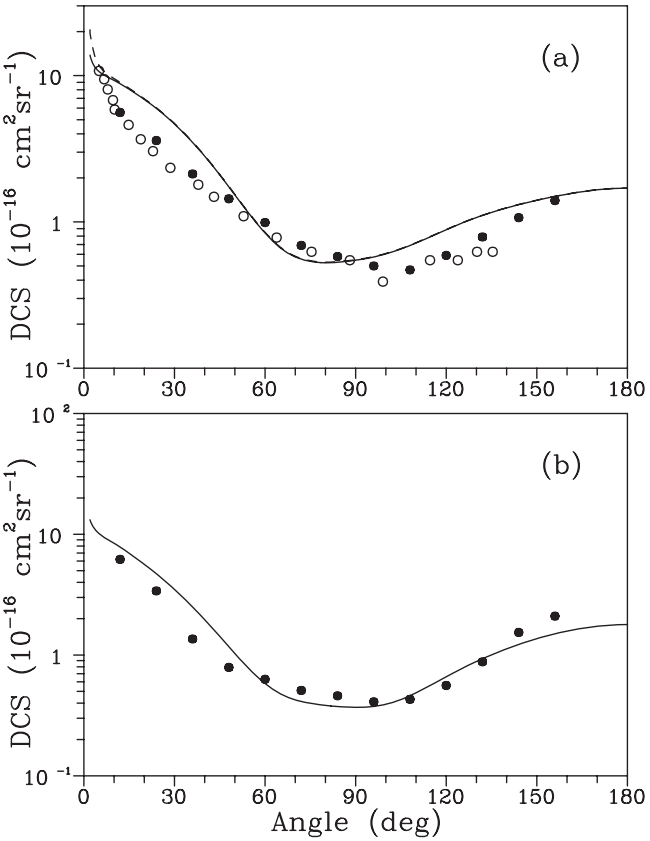

FIG. 4. Same as in Fig. 1, but for (a) 15 eV and (b) 20 eV.

tion [31]. The latter can be conveniently partial-wave expanded as

$$T = \frac{1}{k} \sum_{p\mu lhl'h'} i^{l-l'} T^{p\mu}_{k,lh;l'h'} X^{p\mu}_{lh}(\hat{k}) X^{p\mu^*}_{l'h'}(\hat{k}_0), \tag{5}$$

where $\hat{k}_0$ and $\hat{k}$ are the linear momentum directions of the incident and scattered electrons in BF, respectively, and $X^{p\mu}_{lh}$ are the symmetry-adapted functions [32], which are expanded in terms of the usual spherical harmonics as follows:

$$X^{p\mu}_{lh}(\hat{r}) = \sum_m b^{p\mu}_{lhm} Y_{lm}(\hat{r}). \tag{6}$$

Here p is an irreducible representation (IR) of the molecular point group, μ is a component of this representation, and h distinguishes between different bases of the same IR corresponding to the same value of l. The coefficients $b^{p\mu}_{lhm}$ satisfy important orthogonality relations and are tabulated for C_{2v} and O_h point groups [32].

The rotationally unresolved DCS's for elastic e^--molecule scattering are calculated through a summation of all rotationally resolved DCS's,

$$\frac{d\sigma}{d\Omega} = \sum_{J'\tau'} \frac{d\sigma}{d\Omega}(J\tau \to J'\tau'). \tag{7}$$

In our calculations, the e^--radical scattering dynamics is represented by a complex optical potential given by

$$V_{opt} = V_{SEP} + iV_{ab}, \tag{8}$$

where V_{SEP} is the real part of the optical potential composed of static (V_{st}), exchange (V_{ex}), and correlation-polarization (V_{cp}) contributions, and V_{ab} is the absorption potential. V_{st} and V_{ex} are obtained exactly from a Hartree-Fock (HF) self-consistent-field (SCF) target wave function. A parameter-free model potential introduced by Padial and Norcross [33] is used to account for the correlation-polarization contributions. In this model, a short-range correlation potential between the scattering and the target electrons is defined in an inner region and a long-range polarization potential in an outer region. The first crossing of the correlation and polarization potential curves defines the inner and the outer regions. The correlation potential is calculated by a free-electron-gas model, derived from the target electronic density according to Eq. (9) of Ref. [33]. In addition, the asymptotic form of the polarization potential is used for the long-range electron-target interaction. Since there are no reported experimental dipole polarizabilities for CF_2, the calculated values at the HF-SCF level are used to generate the asymptotic form of V_{cp}. No cutoff or other adjusted parameters are needed for the calculation of the correlation-polarization contribution.

The absorption potential V_{ab} is that of the quasi-free scattering model (QFSM) version 3 of Staszewska *et al.* [34], given by,

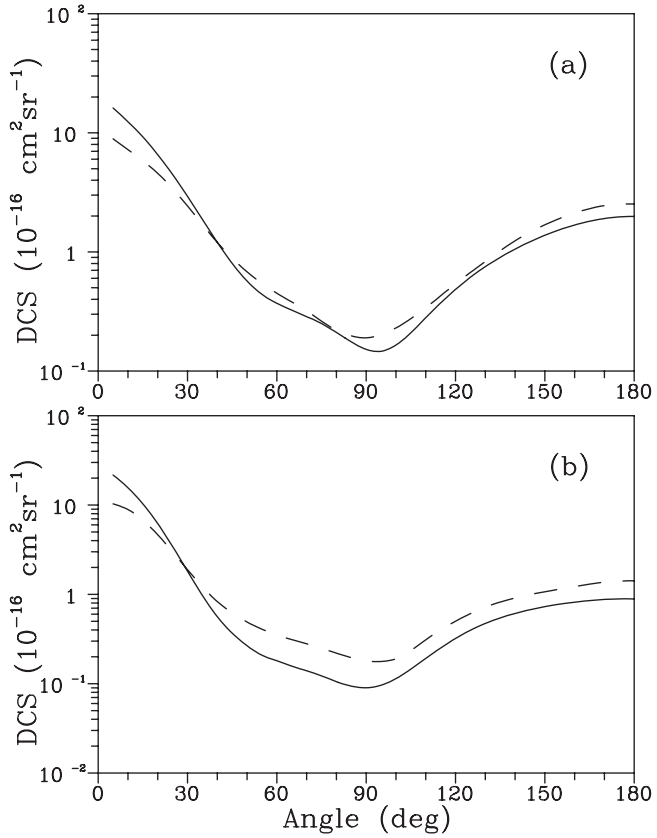

FIG. 5. Same as Fig. 1 but for (a) 30 eV and (b) 50 eV. Long-dashed line: calculated results of Lee *et al.* [29] for e^--O_3 scattering.

$$V_{ab}(\vec{r}) = -\rho(\vec{r})\left(\frac{T_L}{2}\right)^{1/2}\left(\frac{8\pi}{5k^2}k_F^3\right)H(\alpha+\beta-k_F^2)(A+B+C), \tag{9}$$

where

$$T_L = k^2 - V_{SEP}, \tag{10}$$

$$A = \frac{5k_F^3}{(\alpha-k_F^2)}, \tag{11}$$

$$B = -\frac{k_F^3[5(k^2-\beta)+2k_F^2]}{(k^2-\beta)^2}, \tag{12}$$

and

$$C = 2H(\alpha+\beta-k^2)\frac{(\alpha+\beta-k^2)^{5/2}}{(k^2-\beta)^2}. \tag{13}$$

In Eqs. (9)–(13), k^2 is the energy (in rydbergs) of the incident electron, k_F is the Fermi momentum, and $\rho(\vec{r})$ is the local electronic density of the target. $H(x)$ is a Heaviside function defined by $H(x)=1$ for $x \geqslant 0$ and $H(x)=0$ for $x<0$. According to Staszewska *et al.* [34],

$$\alpha(\vec{r},E) = k_F^2 + 2(2\Delta - I) - V_{SEP}, \tag{14}$$

and

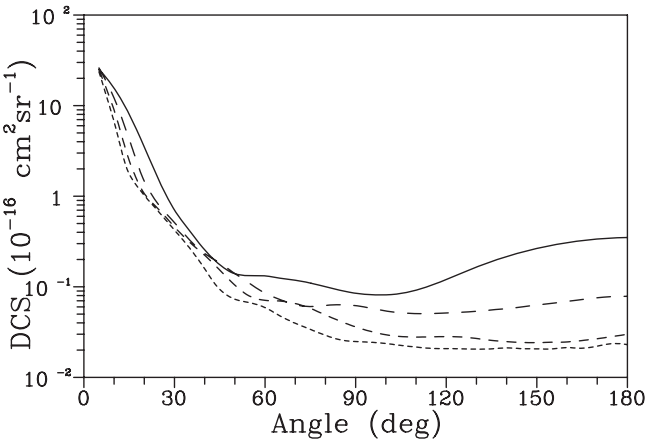

FIG. 6. Present calculated DCS's for elastic e^--CF_2 scattering. Full curve: at 100 eV; dashed line: at 200 eV, short-dashed line: at 300 eV; dotted line: at 400 eV.

$$\beta(\vec{r},E) = k_F^2 + 2(I-\Delta) - V_{SEP}, \tag{15}$$

where Δ is the average excitation energy and I is the ionization potential.

The Lippmann-Schwinger scattering equation for elastic e^--CF_2 collision is solved using the ISVM. In principle, this equation should be solved with the full complex optical interaction potential. Nevertheless, a tremendous computational effort would be required, particularly due to the large number of coupled equations involved, which makes such calculations practically prohibitive. On the other hand, our calculation has revealed that the magnitude of the imaginary part (absorption) of the optical potential is considerably smaller than its real counterpart. Therefore, in the present study the scattering equations are solved using the ISVM, considering only the real part of the optical potential. In ISVM calculations, the continuum wave functions are single-center expanded as

$$\chi_k^{\pm}(\vec{r}) = \left[\frac{2}{\pi}\right]^{1/2}\sum_{lm}\frac{(i)^l}{k}\chi_{klm}^{\pm}(\vec{r})Y_{lm}(\hat{k}), \tag{16}$$

where the superscripts $(-)$ and $(+)$ denote the incoming-wave and outgoing-wave boundary conditions, respectively. Furthermore, the absorption part of the T matrix is calculated via DWA as

$$T_{ab} = i\langle\chi_f^-|V_{ab}|\chi_i^+\rangle, \tag{17}$$

where χ_f^- and χ_i^+ are distorted wave functions calculated in the ISVM. Additionally, the TCS's are calculated by using the optical theorem [35].

In our calculations, the partial-wave expansion of the continuum wave functions as well as of the T-matrix elements are limited to $l_{max}=23$ and $m_{max}=23$. Since CF_2 is a polar system, these partial-wave expansions converge slowly due to the long-range dipole interaction potential. Therefore, a Born-closure formula is used to account for the contribution of higher partial-wave components to the scattering amplitudes. Accordingly, Eq. (5) is rewritten as

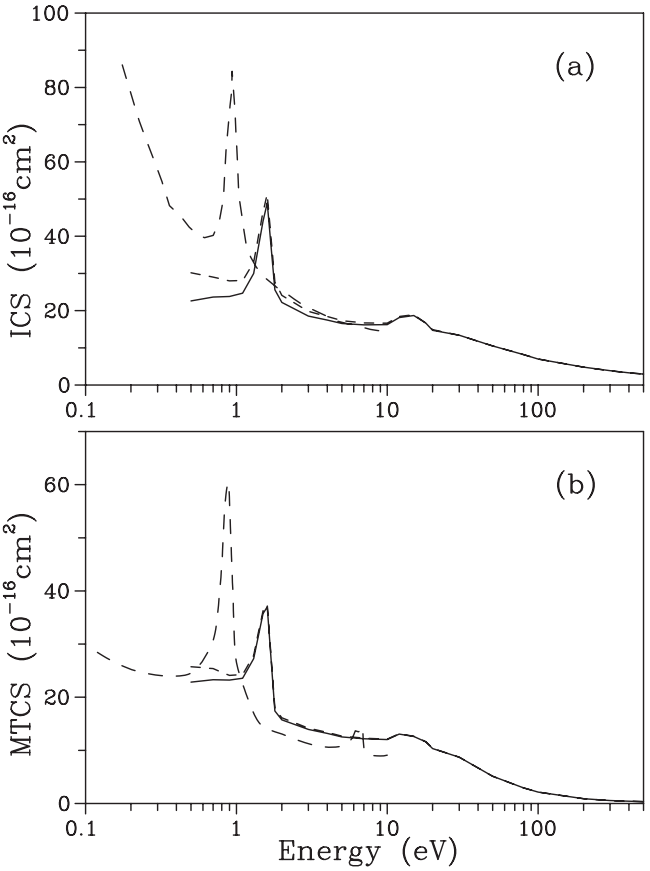

FIG. 7. (a) ICS's and (b) MTCS's for elastic e^--CF_2 scattering. Full curve: present rotationally summed results using the theoretical dipole moment; short-dashed line: present results calculated using the experimental μ; dashed line: calculated DCS's of Rozum and Tennyson [7] using the *R*-matrix method.

$$T = T^B + \frac{1}{k}\sum_{p\mu lhl'h'}^{LL'} i^{l-l'}(T^{p\mu}{}^{ISVM}_{k,lh;l'h'} - T^{p\mu}{}^{B}_{k,lh;l'h'})X^{p\mu}_{lh}(\hat{k})X^{p\mu}{}^{*}_{l'h'}(\hat{k}_0), \tag{18}$$

where T^B is the complete point-dipole first-Born-approximation (FBA) T matrix, $T^{p\mu}{}^{ISVM}_{k,lh;l'h'}$ are the partial-wave T-matrix elements calculated via ISVM, and $T^{p\mu}{}^{B}_{k,lh;l'h'}$ are the corresponding partial-wave point-dipole FBA T-matrix elements, given by

$$T^{p\mu}{}^{B}_{k,lh;l'h'} = -\frac{\mu}{L}\left[\frac{(L+h)(L-h)}{(2L+1)(2L-1)}\right]^{1/2}, \tag{19}$$

where μ is the target electric dipole moment and $L=l'$ when $l'=l+1$ and $L=l$ when $l'=l-1$.

In this study, a standard $[10s5p/4s3p]$ basis set of Dunning [37], augmented by three s (α=0.0473, 0.0125, and 0.0045), four p (α=0.1654, 0.0365, 0.0125, and 0.0035), and three d (α=0.626, 0.15, and 0.0375) uncontracted functions for carbon and three s (α=0.121, 0.0403, and 0.0121), two p (α=0.0913 and 0.033), and one d (α=1.580) uncontracted functions for fluorine, is used for the calculation of the SCF target wave function. At the experimental equilibrium geometry of the ground-state CF_2 (1.304 Å for C-F bond length and 104.8° for the FCF angle), this basis set yielded the calculated SCF energy of −236.7305 a.u., in good agreement with the HF results of −236.7275 a.u. of Russo *et al.* [38]. The calculated dipole moment is 0.246 D, too small when compared with the experimental value of 0.469 D [36]. This discrepancy is probably due to the Hartree-Fock method used in the present study. The electronic correlation effect is very important in the calculation of the reliable dipole moment μ of molecules. In fact, calculated values of μ using more sophisticated methods are 0.44 D [38] and 0.448 D [7], in better agreement with the experimental value. Despite that, our calculated μ of 0.246 D is used to compute the point-dipole FBA T-matrix elements in order to avoid the mismatching between the partial-wave T-matrix elements calculated using the ISVM and FBA. Besides, studies on the influence of the discrepancy between the theoretical and experimental values of μ on the calculated cross sections are also carried out and will be presented in the following section.

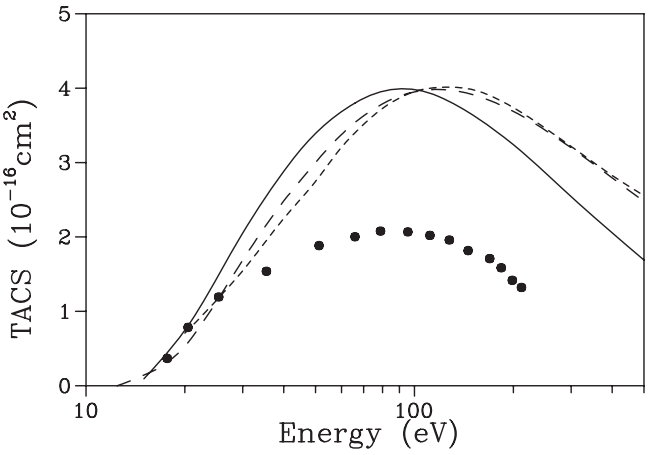

FIG. 8. TACS's for e^--CF_2 scattering in the 15–500 eV range. Full curve: present calculated results, dashed line: BEB TICS's of Kim and Irikura [39]; short-dashed line: calculated results of Antony *et al.* [5]; full circles: experimental TICS's of Deutsch *et al.* [1].

In addition, the TACS's were obtained as the difference between calculated TCS's and ICS's.

III. RESULTS AND DISCUSSION

In Figs. 1–5 we present our calculated rotationally summed DCS's for elastic e^--CF_2 scattering in the 2–50 eV energy range. Unfortunately, there is a lack of experimental investigations on electron interactions with this molecule; therefore we compare our data with the only theoretical DCS's for this target [11] at some limited incident energies. Since CF_2 and O_3 are isoelectronic molecules, calculated [29] and experimental [27,28] results for elastic e^--O_3 collisions are also shown for comparison. In general, our DCS's in the (2–4) eV range are in good qualitative agreement with the corresponding *R*-matrix data of Rozum and Tennyson

[11]. Quantitative agreement is also fair. In addition, there is a general good agreement between our calculated DCS's for CF_2 and the experimental results of Shyn and Sweeney [27] and Allan *et al.* [28] for elastic e^--O_3 scattering, particularly in the (5–20) eV energy range. This good agreement is quite interesting. In this low-energy range, the collision dynamics is dominated by the long-range interactions of both permanent and/or induced dipolar natures as well as by the interaction between the scattering electron and the outer valence electrons of the targets. The fact that CF_2 and O_3 are isoelectronic and both moderately polar has probably contributed to the similar electron-scattering DCS's, both in shape and magnitude, of the two targets. In some way, this good agreement can also indicate the reliability of the present study. At higher energies, the penetration power of the scattering electron into the target electronic clouds increases. In such situations, the interaction of the scattering electron with inner-shell electrons and with nuclei also becomes relevant and thus major differences between the electron scattering DCS's of CF_2 and O_3 may appear, as can be seen in Fig. 5. Particularly, the discrepancy between the DCS's of the two targets presented in this figure is also originated from different levels of approximation used in the description of the collision dynamics. The calculations of Lee *et al.* [29] for O_3 are at the exact static-exchange potential level, whereas correlation-polarization and absorption effects are also accounted for in the present study. In order to investigate the effect of the use of different dipole moments on the cross sections calculated with the Born-closure procedure, DCS's were also calculated using the experimental value of μ. The results obtained at 2 and 15 eV are presented in Figs. 1(a) and 4(a), respectively. Despite the mismatch in the partial-wave expansions of the *T*-matrix elements calculated using the ISVM and FBA, no unphysical structures were introduced in the calculated DCS's when the experimental μ is used in the calculations. Basically, the use of a larger dipole moment enhances the DCS's near the forward direction, but has almost no effect on the DCS's elsewhere. Also, as expected, the discrepancy between the calculated DCS's using different dipole moments decreases rapidly with increasing energy.

In Fig. 6, we present our calculated DCS's in the (100–400) eV energy range. Unfortunately, there is no theoretical or experimental data, even for O_3 to be compared with our results. At such high incident energies, the short-range interactions, particularly with the nuclei, become more important. Therefore, diffraction patterns characterized by regular oscillations begin showing up in the DCS's curves and are more evident at 300 and 400 eV.

Figures 7(a) and 7(b) present our ICS's and MTCS's, respectively, calculated in the (0.5–500) eV range, along with the calculated results of Rozum *et al.* [7,10] for energies up to 10 eV. Again, calculations were also carried out using the experimental value of μ and the results are also shown for comparison. It is seen that the use of a larger dipole moment has affected the magnitude of cross sections only at very low incident energies. On qualitative aspects, our study has shown the existence of a strong shape resonance in both ICS's and MTCS's, located at around 1.5 eV. An eigenphase sum analysis has revealed that the resonance is due to the $^2B_1$ scattering channel, which probably corresponds to the same resonance seen in the cross sections of Rozum *et al.*, but slightly shifted to higher incident energies. Also, our calculated resonance is less intense (48.9 and 37.0 $Å^2$ at the maxima of ICS's and MTCS's, respectively) than theirs (around 82 and 60.4 $Å^2$ at the corresponding maxima). Both the position and width of low-energy shape resonances are very sensitive to the details of the interaction potentials. Therefore, the observed discrepancy may be due to the different target wave functions used to generate static-exchange potentials, to the different manner to account for correlation-polarization contributions, as well as to the different partial-wave truncations used in both calculations. Moreover, some structures shown in their MTCS's between 6 and 7 eV incident energies are neither seen in their ICS's nor in our ICS's and MTCS's. In addition, our calculation revealed another resonance, located at around 15 eV, which has been associated to the $^2B_2$ scattering channel. Quantitatively, our calculated ICS's agree quite well with the *R*-matrix data of Rozum *et al.* [7] at incident energies away from the resonance region (above 2 eV). The agreement between our and their MTCS's is also quite reasonable in the same energy region. Nevertheless, their calculated results show a fast increase with the decrease of incident energies towards threshold, not seen in our calculated data. This discrepancy can be partially explained by the too small dipole moment used in our calculation. Indeed, the ICS's obtained with the experimental μ has already shown a trend to such an increase. Therefore, we expect that this behavior of our calculated ICS's and MTCS's would certainly show up, but at much lower energies.

Figure 8 shows our calculated TACS's in the 15–500 eV energy range for the e^--CF_2 collisions. Experimental TICS's of Deutsch *et al.* [1], TICS's calculated using the binary-encounter Bethe (BEB) model of Kim and Irikura [39], and those calculated by Antony *et al.* [5] using the group additivity method are also shown for comparison. In general, there is a good qualitative agreement between the present calculated TACS's and the results available for comparison. Quantitatively, our calculated TACS's agree reasonably well with the BEB TICS's of Kim and Irikura, as well as with those of Antony *et al.* However, all theoretical results lie well above the experimental TICS's of Deutsch *et al.* [1]. In fact, our calculated TACS's account for both excitation and ionization processes and therefore they are an upper limit of the TICS's. If we assume that the ionization contribution is about 80% in the energy range covered herein, our TACS's are still too large in comparison with the experimental data. Taking a close look in the literature, we noticed that the BEB calculations are capable of providing TICS's in very good agreement with experiments for some stable carbon perfluoride species with the generic formula C_nF_{2n+1} $(n=1,2,3)$ [40]. On the other hand, that model has systematically overestimated experimental TICS's by roughly a factor of 2, for

reactive carbon fluoride radicals CF_x ($x=1,2,3$) [39]. Therefore, it is possible that the existing theoretical models are still unable to describe adequately the interaction of an electron with such species. Nevertheless, there are also possible experimental difficulties in the measurement of TICS's for such highly reactive radicals. The experimental data of Deutsch *et al.* [1] is the only one available in the literature. Therefore, more experimental efforts are welcome in order to clarify this discrepancy.

ACKNOWLEDGMENTS

This work was partially supported by the Brazilian agencies FAPESP, CNPq, and FINEP-PADCT.

[1] H. Deutsch, T. D. Märk, V. Tarnovsky, K. Becker, C. Cornelissen, L. Cespiva, and V. Bonacic-Koutecky, Int. J. Mass Spectrom. Ion Process. **137**, 77 (1994).
[2] V. Tarnovsky, P. Kurunkczi, D. Rogozhinikov, and K. Becker, Int. J. Mass Spectrom. Ion Process. **128**, 181 (1993).
[3] R. B. Diniz, M. A. P. Lima, and F. J. da Paixão, J. Phys. B **32**, L539 (1999).
[4] M.-T. Lee, I. Iga, L. M. Brescansin, L. E. Machado, and F. B. C. Machado, Phys. Rev. A **66**, 012720 (2002).
[5] B. K. Antony, K. N. Joshipura, and N. J. Mason, J. Phys. B **38**, 189 (2005).
[6] K. N. Joshipura and M. Vinodkumar, Z. Phys. D: At., Mol. Clusters **41**, 133 (1997).
[7] I. Rozum, N. J. Mason, and J. Tennyson, J. Phys. B **35**, 1583 (2002).
[8] I. Rozum, N. J. Mason, and J. Tennyson, New J. Phys. **5**, 155 (2003).
[9] I. Rozum, N. J. Mason, and J. Tennyson, J. Phys. B **36**, 2419 (2003).
[10] I. Rozum, P. Limao-Vieira, S. Eden, J. Tennyson, and N. J. Mason, J. Phys. Chem. Ref. Data **35**, 267 (2006).
[11] I. Rozum and J. Tennyson, J. Phys. B **37**, 957 (2004).
[12] B. K. Sarpal, K. Pfingst, B. M. Nestmann, and S. D. Peyerimhoff, Chem. Phys. Lett. **230**, 231 (1994).
[13] B. K. Sarpal, B. M. Nestmann, and S. D. Peyerimhoff, J. Phys. B **31**, 1333 (1998).
[14] R. Gulley, T. A. Field, W. A. Steer, N. J. Mason, S. L. Lunt, J.-P. Ziesel, and D. Field, J. Phys. B **31**, 5197 (1998).
[15] R. R. Lucchese, G. Raseev, and V. McKoy, Phys. Rev. A **25**, 2572 (1982).
[16] L. Mu-Tao, L. M. Brescansin, M. A. P. Lima, L. E. Machado, and E. P. Leal, J. Phys. B **23**, 4331 (1990).
[17] A. W. Fliflet and V. McKoy, Phys. Rev. A **21**, 1863 (1980).
[18] M.-T. Lee and V. McKoy, Phys. Rev. A **28**, 697 (1983).
[19] Mu-Tao Lee, S. Michelin, L. E. Machado, and L. M. Brescansin, J. Phys. B **26**, L203 (1993).
[20] M.-T. Lee, I. Iga, L. E. Machado, and L. M. Brescansin, Phys. Rev. A **62**, 062710 (2000).
[21] M.-T. Lee and I. Iga, J. Phys. B **32**, 453 (1999).
[22] L. E. Machado, E. M. S. Ribeiro, M.-T. Lee, M. M. Fujimoto, and L. M. Brescansin, Phys. Rev. A **60**, 1199 (1999).
[23] I. Iga, M. G. P. Homem, K. T. Mazon, and M.-T. Lee, J. Phys. B **32**, 4373 (1999).
[24] S. E. Michelin, T. Kroin, I. Iga, M. G. P. Homem, and M.-T. Lee, J. Phys. B **33**, 3293 (2000).
[25] K. N. Joshipura, M. Vinodkumar, and P. M. Patel, J. Phys. B **34**, 509 (2000).
[26] L. G. Christophorou and J. K. Olthoff, J. Phys. Chem. Ref. Data **28**, 967 (1999).
[27] T. W. Shyn and C. J. Sweeney, Phys. Rev. A **47**, 2919 (1993).
[28] M. Allan, K. R. Asmis, D. B. Popovic, M. Stepanovic, N. J. Mason, and J. A. Davies, J. Phys. B **29**, 4727 (1996).
[29] M.-T. Lee, S. Michelin, T. Kroin, and L. E. Machado, J. Phys. B **31**, 1781 (1998).
[30] A. Jain and D. G. Thompson, Comput. Phys. Commun. **30**, 301 (1983).
[31] M. E. Rose, *Elementary Theory of Angular Momentum* (John Wiley & Sons, New York, 1957).
[32] P. G. Burke, N. Chandra, and F. A. Gianturco, J. Phys. B **5**, 2212 (1972).
[33] N. T. Padial and D. W. Norcross, Phys. Rev. A **29**, 1742 (1984).
[34] G. Staszewska, D. W. Schwenke, and D. G. Truhlar, Phys. Rev. A **29**, 3078 (1984).
[35] C. J. Joachain, *Quantum Collision Theory* (North Holland, Amsterdam, 1983).
[36] W. H. Kirchhoff, D. R. Lide, Jr., and F. X. Power, J. Mol. Spectrosc. **47**, 491 (1973).
[37] T. H. Dunning, Jr., J. Chem. Phys. **53**, 2823 (1970).
[38] N. Russo, E. Sicilia, and M. Toscano, J. Chem. Phys. **97**, 5031 (1992).
[39] Y.-K. Kim and K. K. Irikura, *Proceedings of the 2nd International Conference on Atom Molecular Data and their Applications*, edited by K. Barrigton and K. L. Bell, AIP Conf. Proc. No. 543 (AIP, New York, 2000), p. 220.
[40] N. Nishimura, W. M. Huo, M. A. Ali, and Y.-K. Kim, J. Chem. Phys. **110**, 3811 (1999).